Comparison and improvement of tangent estimators on digital curves ⋆

François de Vieilleville and Jacques-Olivier Lachaud [a,b,*]

[a] *SUNY State college at Buffalo,*
Bishop Hall,1300 Elmwood street, Buffalo, NY, 1500-1333

[b] *Laboratoire de Mathématiques, UMR CNRS 5127*
Université de Savoie, 73776 Le-Bourget-du-Lac, France

Abstract

Many contour-based applications rely on the estimation of the geometry of the shape, such as pattern recognition or classification methods. This paper proposes a comprehensive evaluation on the problem of tangent estimators on digital curves. The methods taken into account use different paradigms : approximation and digital geometry. In the former paradigm, methods based on polynomial fitting, smoothing and filtering are reviewed. In the latter case of digital geometry, we consider two methods that mainly rely on digital straight line recognition [13] and optimization [9]. The comparison takes into account objective criteria such as multi-grid convergence, average error, maximum error, isotropy and length estimation. Experiments underline that adaptive methods based on digital straight line recognition often propose a good trade-off between time and precision and that if precision is to be sought, non-adaptive methods can be easily transformed into adaptive methods to get more accurate estimations.

Key words: digital straight segments, tangent estimator, adaptive tangent estimator, multi-grid convergence

1. Introduction

The proper detection of significant features along digital curves often relies on an accurate estimation of the geometry of the supposed underlying curve. Local geometric quantities such as curvature and tangent orientation lead naturally to the detection of dominant points on digital curves [22,18]. Moreover some geometric quantities may almost be used directly to compute another quantity: tangent estimation provides length estimation by simple integration. In fact the accurate comparison and estimation of local geometric quantities on digitized shapes rely on four tasks:

(1) Find an Euclidean continuous shape as the reference for a given digitized shape.
(2) Determine the size of the computation window to achieve the best possible estimation at a given digital point.
(3) Estimate noise or distortion of the digitized curve.
(4) Compute the result as fast as possible.

The first problem requires additional hypotheses to define a reference shape for a given digital shape, properties such as smoothness, compactness, convexity, minimal perimeter or maximal area are common choices. For instance, given a digital disk, a reasonable hypothesis is that the underlying shape is an Euclidean disk, and not some kind of gears with small cogs. The second problem involves the adaptability of computation windows to the local geometry of the shape, e.g. curves with huge curvature variations require different sizes for the computation windows. Sizes of computation windows are known to have an important impact on the multi-grid convergence (see [5]). The third problem is a common problem which is efficiently addressed in the continuous world, but lacks proper definitions in the digital world. This entails that continuous methods are generally preferred for the extraction of geometric quantities. The fourth problem arises when the computation windows are too large, while narrowing their sizes has a direct impact on the precision of the method. These issues are related to many interesting topics on digital geometry such as multi-grid convergence [3,11], digitization problems and topology issues [15], combinatorial properties of digitized shapes [1] and new models for digital straight segments taking into

⋆ This work is funded by the ANR Géodib Project and Lavoisier fellowship.
* Corresponding author.
Email address: devieill@math.buffalostate.edu (François de Vieilleville and Jacques-Olivier Lachaud).

account some distortions [6].

As mentioned earlier usual geometric estimators are based on approximation techniques in the continuous Euclidean space. They forget the particularities of subsets of the digital plane. Doing so, they address problem (3) considering that it is the main issue. The noise is then handled by tuning some external parameters. In fact the external parameters often reduce to the choice of the size of the computation window, handling problems (2), (3) and (4) at the same time with a trade-off. The continuous methods can be of various type with different aims with respect to the digital curve: interpolation, reconstruction or fit. The choice of the underlying curve in problem (1) is then often made explicitly with the method itself, e.g. using cubic splines to interpolate points along a digital curve lead to degree three polynomials as the underlying curve. The numerical methods required to extract the chosen solution can be costly and may even require parameters themselves. This is particularly true when the chosen underlying curve is the solution of a non trivial optimization problem. As a result problem (1) and (2) have a direct impact on (4).

On the contrary, standard digital estimators based on digital straight segment recognition estimate local geometric quantities like tangent or curvature with an adaptive computation window and, at the same time, they do not require any external parameters [7,12,24]. Recently, an evaluation of digital tangent estimators was performed in [12] and the λ-MST was shown to outperform the others on many criteria like precision, maximal error, isotropy, convergence, convexity on ideal digital shapes (with very little noise). The tangent orientation is determined using digital straight segment recognition, which entails a computation window adapted to the local curve geometry (addressing problem (2)) and without assumptions on the underlying curve (addressing problem (1)). For large families of shapes the average size of the computation window is known and is roughly in $\Theta\left(h^{-1/3}\right)$ where h is the grid step (see [5] for technical proofs). As a result, the asymptotic convergence — or multi-grid convergence — of the λ-MST estimator is proved for smooth and convex curves [13]. This estimator is also the best among digital ones at rough scale [12,13]. Its computation on the whole digital curve, i.e. the computation of the tangent orientation field, may be done in time linear with the number of digital points (optimal time, addressing (4)). This estimator has already been shown to be as good as standard continuous methods [4].

This paper aims first at describing objective criteria for the tangent estimation on various suitable representatives types of digital curves. Among them we consider the problem of detecting false concavities on the estimation of convex shapes. Time benchmarks are also taken into account for the computation of the tangent orientation field. Moreover the multi-grid convergence criteria are also considered using various aspect: the average absolute error is considered but also the maximal absolute error. Furthermore we use criteria mixing the preceding ones to better reflect the possible trade-off expected when estimating the tangent orientation field.

Besides, our aim is not only to compare estimators but also to see if they can benefit from one another. This is the case here where we show how non-adaptive methods can become adaptive to the local geometry using digital straight segment recognition. The obtained improvements are illustrated experimentally and discussed. Moreover the use of our digital primitive allow us to prove the multi-grid convergence for one of the proposed adaptive method using the Gaussian derivative. All these experiments indicate that there is no estimator outperforming the others on every objective criteria.

The paper is organized as follow. First we describe the objective criteria that will be used to discriminate the tangent estimators and the suitable shapes that should be used to run our experiments. We also elaborate on our framework to explain how do we compare the estimated values with the expected ones. In Section 3 we review the continuous tangent estimator based on approximation and at a later time the digital ones. In Section 4 we conduct experiments following the objective criteria proposed in Section 1. An objective criterion called AAEBT taking into account precision and time computation at the same time shows that techniques based on digital straight segments are very appealing. In Section 5, we propose improvements for the non-adaptive methods, which are underlined experimentally, especially regarding the precision criteria. For one them, its multi-grid convergence is proved. These experiments clearly show how much the precision improves when the classical methods use an adaptive neighborhood and often yield a very good possible precision. However these precision improvements have a cost in terms of time and these hybrid estimators would be considered average regarding the AAEBT criterion. Our conclusion is thus that digital straight segments are a very powerful tool to analyze locally the geometry of digital curves and to get the proper adaptive computation windows for estimating the characteristics of the underlying shape without *a priori* knowledge.

2. Criteria and Shapes Used for Comparison

In this section we elaborate on the different objective criteria chosen for this study and what they reflect. As a consequence we describe the different test shapes corresponding to our chosen objective criteria. The experimental protocol is also described.

2.1. *Objective Criteria*

In a general context, the efficiency of an estimator is mainly measured by its precision, that is the less difference with the theoretical value, the better. Due to problem (1), one of the best way to measure the efficiency of an estimator is to use the *multi-grid convergence*: that is, for a given shape, to measure the deviation between the theoretical value and the estimated value as a function of the in-

verse of the grid step. This allows us to answer experimentally to the question "Does a finer resolution yields a better precision ?". As experiments cannot be conducted on all shape, representative ones have to be taken into account. Since very large resolutions are considered, their digitizations will mainly depend on their curvature. Thus we need shapes that would reflect the possible curvature variations. As a consequence choose to focus on constant curvature, smooth variations between two positive bounds and strong variations between opposite signed bounds. On the other hand the precision of the estimator is measured with the average absolute error (AAE) or the maximal error (ME) on the whole digital shape. These two criteria reflect the general and the worst behaviour of the estimator. Although we do not consider noise in this study, we consider for each resolution fifty random shifts of the center of the Euclidean shape (in a square whose side equals that of the grid step) before its digitization so as to introduce some small variations in the considered digital shapes.

Other objective criteria for estimators address general properties of the shape. Of course, as estimators work on digitizations, not all the properties of the underlying shape are meaningful. Nonetheless we consider that the convexity is a remarkable property that should be kept by estimators, as the digitization preserves it. As a result if an estimator creates false inflexion points or concavities on the digitization of a convex shape, it is considered as a severe defect. Furthermore properties of a local estimator in the digital space compared to the expected properties in the Euclidean space are relevant for discriminating estimators. Thus properties such as isotropic behaviour have to be evaluated in order to choose reliable estimators. Such evaluation is to be conducted on the most regular shape possible regarding the directions in the Euclidean plane. Let us also note that in Euclidean geometry many geometric quantities are related to each other, for example the tangent along the curve leads directly to length computation by integration. As a result the tangent estimation should lead to good length estimation provided the isotropic behaviour of the estimator does not penalizes it too much. Thus the shape chosen for the evaluation of the perimeter has to minimize the influence of the isotropic behaviour and has to be as regular as possible in the possible direction of the Euclidean space.

The other usual criterion used for comparison is the time spent on computation. This quantity can in fact also be measured as a function of the grid step, enabling the formulation of mixed criteria taking into account precision and time. The product of the AAE by the time spent on computation lead to another objective criteria for the performance of an estimator, called AAEBT, balancing precision and time as a function of the inverse of the grid step.

2.2. *Test Shapes and Experimental Protocol*

The considered shapes reflect the various comparison needs for the evaluation of the tangent estimators. As mentioned above, we chose curves from their curvature as follows: for the constant curvature we choose a circle, for smooth variations of the curvature we choose an ellipse and for strong variations with sign changes we choose a flower. More precisely the chosen ellipse has a curvature variation between 0.49 and 1.42857, and the flower between 5.8 and -26.1, with five inflexion points. The defects of estimators regarding the convexity analysis are done on the border of the digitization of a disk, near points corresponding to a quadrant change. For the isotropy behaviour and the perimeter estimation, the best possible shape is the circle, as it is the most regular shape in all directions of the Euclidean plane. Nonetheless for this experiments the number of random shifts of the center of the shape before the digitization process will be increased to 100. Indeed, from a theoretical point of view there is essentially $4\pi^2R^2$ different Gauss digitizations of a disk of radius R (see [8]), with grid step equals to one, thus requiring more variations in order to have a representative set of digital disks.

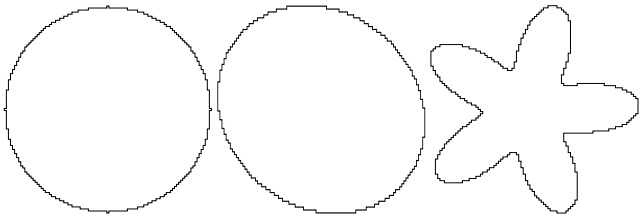

Fig. 1. Borders of Gauss digitizations with grid step equal to 0.02 for the proposed test shapes. (Left) Shape is a circle of radius 1. (Middle) Shape is an ellipse with half-great axis equal to 1.0 and a half-small axis equal to 0.7, rotated by 0.2 radian. (Right) Shape is a flower with five branches, outer radius 1.0 and inner radius 0.4 rotated by 0.2 radian.

Of course we do not work directly on Euclidean shapes but on the border of digitized shapes. We use the Gauss digitization (that is the intersection of the Euclidean shape with the digital plane, up to a factor representing the grid step) and then extract the digital border using cell decomposition. Border of the proposed digitized shapes are illustrated on Fig. 1.

In the remaining of the paper the considered digital curves are digital 4-curves, that is a 4-connected closed sequence of points in $\mathbb{Z}^2$ such that each of them has exactly two 4-neighbors: a predecessor and a follower (given an orientation). Such curves arise naturally from the cellular decomposition (putting it simply the inter-pixel contour) of the Gauss digitization of simple Euclidean objects, provided they are well-composed [14]. In our framework we consider that the digital border of a shape is made of *linel* (which can also be seen as the so-called Freeman moves), that is the side of a square whose center has the coordinates of a digital point. The obtained digital curve is denoted C and its elements are ordered increasingly with a counterclockwise order, C_i denotes the i-th linel of the digital curve or its centroid and $C_{i,j}$ is the digital path from the i-th linel to the j-th linel.

On the digital border of a shape, for a given linel/point

it is difficult to find a point on the continuous border to compare with. When dealing with the absolute deviation of the tangent orientation, our theoretical value is obtained by averaging the theoretical orientations that lies on the border of the continuous shape within the projected endpoints of the linel of interest (from the origin); see Fig. 2 for an illustration. This enable us to compare the estimated value with a representative theoretical value for the linel of interest. On the other hand, when dealing with the maximal absolute deviation on a linel, our theoretical value is the one that maximize the absolute error within the projected endpoints of the linel of interest on the border of the continuous shape. Again this method allows us to have a representative maximal error. Such methods are much easier when using polar coordinates. Eventually the tangent orientation at a given point will be measured as the angle between the vector $(1, 0)$ and the one obtained from the estimation of the derivative at the given point.

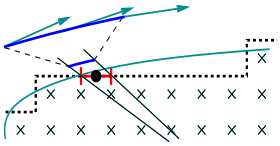

Fig. 2. Illustration of the comparison between estimated value and theoretical value. The border of the underlying curve is drawn with solid line, points of the digital shape are marked with a black cross. The border of the digital shape is drawn with dashed line and the linel of interest is drawn as a segment with bracket. The point of estimation is drawn with a small circle in black, in blue the points chosen for computing an average value from the theoretical values of the underlying curve.

3. Continuous and Discrete Tangent Estimators

This section presents the three continuous methods and the two discrete methods that are considered in this study.

3.1. *Continuous Estimators*

The three continuous method used need an external parameter to achieve the best possible accuracy: the size of the computation window.

3.1.1. *Least square methods using polynomials*

The aim of these methods is to find a polynomial of finite degree which minimizes a positional squared error from a set of samples. More precisely, let us denote by $(s_i = (x_i, y_i))_{1 \leq i \leq M}$ a set of M samples obtained from a planar curve parametrized as $y = f(x)$. We thus seek to minimize the functional $E(a_0, \ldots, a_N) = \sum_{i=1}^{M} \left(y_i - \sum_{j=0}^{N} a_j x_i^j \right)^2$.

The simplest form of this quantity is when N equals one and is called a linear regression. In the general case, the problem can be reduced to a matrix inversion problem. At least one solution exists and can be efficiently computed using QR factorisation [21]. For small degree polynomials, direct computation is possible as it involves square matrices of order two and three. It is not compulsory that the polynomial be the supposed underlying curve itself. It can also be its local Taylor expansion as explained in [16] for implicit parabola fitting, an approach which is generalized by the *n-jets* of [2].

Once the optimal polynomial for E is determined, the coefficient associated to its X monomial may be used to estimate the tangent orientation. We naturally focus on low order polynomials. That is the linear regression (LR, Eq. (1)), implicit parabola fitting (IPF, Eq. (2)), and explicit parabola fitting (EPF, Eq. (3)). When used for approaching the tangent orientation at the point of interest C_0, considered as the origin, with a computation window ranging from C_{-q} to C_q, those three methods give very similar results (see Figure 3).

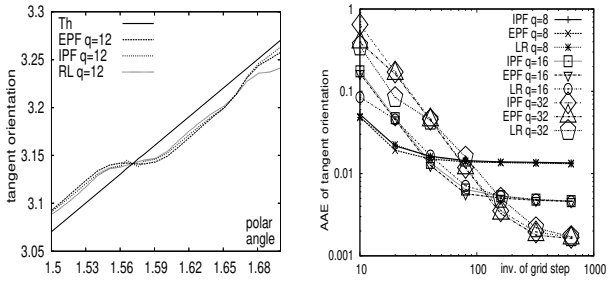

Fig. 3. We represent the tangent orientation estimated with IPF,EPF and LR methods. The test shape is a circle of radius 1. Computation window equals $2q+1$. (Left) Grid step equals 0.01, we focus on a part of the shape, x-axis represents the polar angle, the y-axis represents the orientation of the tangent. (Right) The plot is in log-space and represent the AAE between true tangent and estimated tangent as a function of the grid step. For each grid step 50 experiments are made with a random shift on the center of the shape.

$$E_{LR}(a, b) = E(a, b, 0, \ldots) \quad (1)$$

$$E_{IPF}(a, b) = E(0, a, b, 0, \ldots) \quad (2)$$

$$E_{EPF}(a, b, c) = E(a, b, c, 0, \ldots) \quad (3)$$

A refinement of this method is the *weighted least square fitting*, where each sample has a variable importance in the fitting process: the heavier the weight, the more important the fit. However, it is not easy to find meaningful weights within our context.

When used with 4-connected contour, the use of *independent coordinates* is a better solution (denoted ICIPF for implicit parabola fitting using independent coordinates), as it does not require to estimate the orientation of the samples. The fit is done on each coordinates with respect to a given parametrization of the curve. Usually centered windows are considered: C_0 is the point of interest, $M = 2q+1$ is the size of the computation window going from C_{-q} to C_q. When using independent coordinates, the arc-length from C_0 to C_i, denoted l_i is computed as $l_i = \sum_{k=0}^{i-1} d_1(C_k, C_{k+1})$ if

$i > 0$ and $-\sum_{k=0}^{i-1} d_1(C_k, C_{k+1})$ otherwise. [1] We are thus interested in minimizing the two following quantities:

$$\sum_{i=1}^{M} \left(x_{C_i} - \sum_{j=0}^{N} a_j l_i^j \right)^2$$
$$\sum_{i=1}^{M} \left(y_{C_i} - \sum_{j=0}^{N} b_j l_i^j \right)^2$$

We hence use the preceding method with the underlying curve parametrized as $(x(s), y(s))$. This *a priori* parametrization can be iteratively refined using the length estimator proposed earlier-on, denoted ITICIPF. Unfortunately, this method does not yield better result, even on a circle (constant curvature) or the flower (fast curvature variation) as shown on Fig. 4. As a result we will only consider the ICIPF method for the comparison with the other estimators.

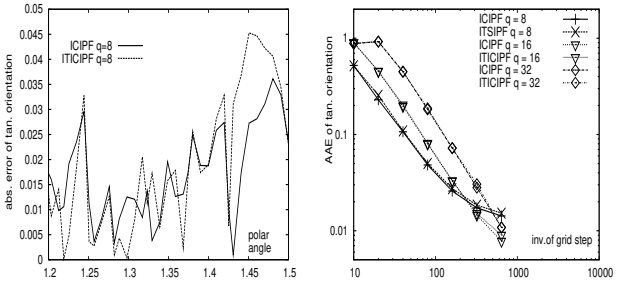

Fig. 4. Plot using the iterative version of ICIPF with ten iterations and the ICIPF. (Left) The test shape is a circle digitized for a grid step equal to 0.01. The iterative ICIPF method using the length estimation is shown not to be better than the ICIPF method, giving very similar values regarding the AAE (0.014855 for the ICIPF and 0.017265 for ITICIPF) and also regarding the ME (0.059590 for the ICIPF and 0.061704 for ITSIPF). (Right) Multi-grid convergence of the ICIPF and the iterative ICIPF with ten iterations, the test shape is a flower, experiments are run in the conditions described earlier-on. As shown on the plot there is little difference between the two methods.

3.1.2. *Smoothing and Filtering*

The use of Gaussian filters is a common technique for improving the quality of noisy images. This filter can also be used when trying to analyze a digital curve, and has been used in the pattern recognition community for almost 30 years. It is essentially a weighted averaging over a finite window. The obtained smoothed continuous curve is considered to be a good approximation of the underlying curve. Its derivatives are easily computed yielding geometric quantities of the first and second order. This reconstruction has one major drawback, which is the choice of the parameter σ. This tuning parameter is often chosen for the whole curve, but it is not satisfying if the curve has huge curvature variations, entailing then over-smoothing for some region and under-smoothing for others. As a result techniques using scale-space were proposed [20,25] to achieve a better localization of the dominant points across the different σ values. From a discrete point of view we will consider that the estimated derivative at the digital point C_0, say $\hat{\mathbf{C}}'_0$, is obtained as: $\hat{\mathbf{C}}'_0 = \sum_{i=-q}^{q} G'_{\sigma_q}(-i)\mathbf{C}_i$, with $\sigma_q = \frac{q}{3}$ and where $G'_\sigma(t)$ is the first derivative of the Gaussian function $G_\sigma(t) = \frac{1}{\sigma\sqrt{2\pi}} \exp\left(\frac{-t^2}{2\sigma^2}\right)$.

We also consider an adaptation of the median filter commonly used in image processing. This method was proposed in [19] and consists in choosing the median orientation among the following $2q$ vectors centered on C_i: $(\mathbf{C_{i-q}C_i}, \ldots, \mathbf{C_{i-1}C_i}, \mathbf{C_iC_{i+1}}, \ldots, \mathbf{C_iC_{i+q}})$ as illustrated on Fig. 5.

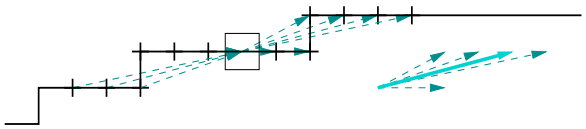

Fig. 5. Illustration of the median filter method. Boxed point is C_i and $q = 6$. Thick arrow represents the chosen tangent orientation at point C_i.

3.2. *Discrete Methods*

This section briefly presents the discrete tangent estimators chosen for this study. The first of them, the λ-MST estimator, relies on DSS recognition, while the GMC estimator rely on curvature through optimisation process.

3.2.1. *The λ-MST tangent estimator*

The λ-MST tangent estimator is based on the digital straight segments of a digital curve, and more particularly the set of inextensible digital straight segments, also called the set of maximal segments. At a given point, this method considers the set of maximal segments passing through the point of interest (see Fig. 6), and estimates the tangent as a convex combination of the orientation of each of these maximal segments. The weights are parametrized by the distance from the point of interest to their center point and further tuned with a function λ. In this study, the function λ is the triangle function. This choice guarantees that the λ-MST estimator satisfies the convexity/concavity property [2], as shown in [13] (see Theorem 8). This estimator also has a good isotropic behaviour, it is uniformly multigrid convergent and the computation of the tangent field can be achieved in time linear with respect to the number of curve points, see [13] for the detail of this properties.

3.2.2. *The GMC Estimator*

The Global Min-Curvature [9] (GMC for short) method is based on a global optimization scheme. Given a digital shape, it finds a continuous shape which minimizes its squared curvature along its boundary, within a family of shapes with the same digitization as the input digital shape. In a way, this method tries to find the smoothest shape

[1] d_1 denotes the distance obtained from the $||\cdot||_1$ norm.

[2] Estimated tangent directions are monotone for digitization of convex shapes.

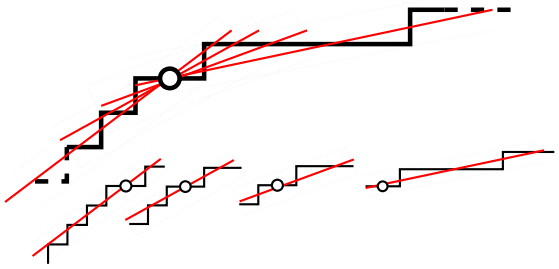

Fig. 6. Set of maximal segments passing through a point on a portion of the digital border of a shape.

whose digitization is the input data, and claims the geometry of this shape provides good geometric estimates for the digital shape. More precisely, the optimization process is casted in the space of tangent directions, where the shape boundary is represented by its tangent direction as a function of the curvilinear abscissa. There, each maximal segment defines local bounds on the possible tangent directions, in order to ensure that the shape has approximately the same Gauss digitization as the input shape. An iterative relaxation scheme numerically extracts the optimal shape within these bounds. After that, the computation of the tangent estimation is straightforward.

4. Experimental evaluation

This section gathers the experiments done with the test shapes described earlier-on, using the criteria proposed in Section 2. The criteria chosen for the evaluation made here on the various estimators is, to our knowledge, as comprehensive as possible.

4.1. *Simple Objective Criteria*

We here review the criteria that do not need multi-grid analysis to reveal the properties of the estimators.

4.1.1. *Concavity/Convexity Detection*

When we consider the digitization of convex shapes, the analysis of its border with a tangent estimator should not lead to false concavity/convexity detection. Though convex shapes can be complicated, we have chosen to show that even on a simple shape such as the circle, whose digitization is always *digitally convex*[3] for grid steps smaller than a constant value, false detection may occur. As shown on Figure 7, for fixed-sized estimators these defects appear very clearly near a quadrant change as huge signed variations of the tangent orientation.

The false convexity/concavity detection can be alleged to a wrong size of the computation window and quadrant changes are not the only parts with such problems : as borders of digitized shapes have straight parts, tangent estimators with small sizes of computation window will estimate either 0, $\pi/2$, π or $3\pi/2$ on such parts. Experimentally on digitized circles it seems that if the size of the computation window exceeds some value being a function of the radius and the grid step, false convexity/concavity points disappear or at least the variations become smaller and smaller. More precisely, this phenomenon is related to the maximal curvature of the shape under study. This defect can be clearly considered as a huge drawback of fixed-size estimators which cannot be overcome unless the maximal curvature of the shape is known *a priori*. As a result tangent estimators using adaptive window size or those taking into account the global geometry of the digitized shape behave much better, with the GMC estimator being clearly the best on this point.

[3] That is 4-connected and equal to the Gauss digitization of its convex hull.

False Concavities Detection On a Digitized Disk

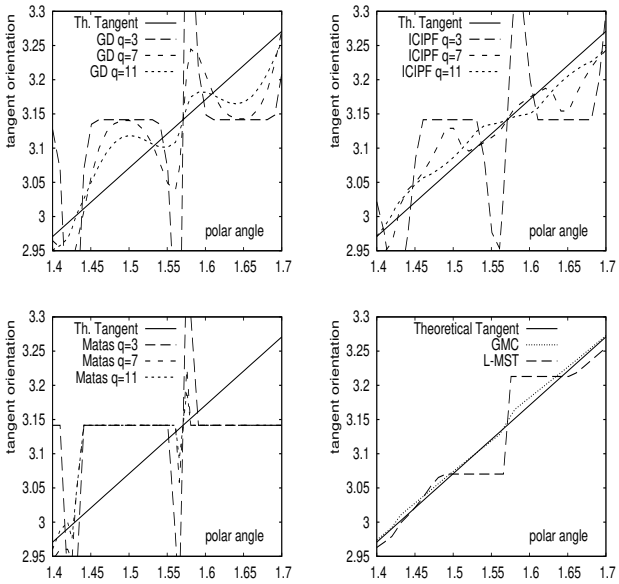

Criterion	GD	ICIPF	MATAS	λ-MST	GMC
Create False Concavities	Yes	Yes	Yes	No	No

Fig. 7. Test shape is a circle of radius 1, digitized with a grid step equal to 0.01. Tangent orientation is plotted as a function of the polar angle. The x-axis represents the polar angle, the y-axis represents the orientation of the tangent and the size of the computation window equals $2q+1$. (Left-top) Tangent orientation obtained using convolutions by the Gaussian derivative σ_q. (Right-top) Tangent orientation obtained using implicit parabola fitting with independent coordinates. (Left-bottom) Tangent orientation obtained using the median filtering. (Right-bottom) Tangent orientation using the λ-MST estimator and the GMC estimator.

4.1.2. *Isotropy Behaviour*

As the digital plane is not isotropic, it is important to check if the methods used to extract geometric information are heavily sensitive to the same problem. To achieve such a study we have chosen to use the circle as a test shape, digitized for a small enough grid step so that its digital boundary is close enough to that of a circle. As shown on Fig. 8, fixed-size estimators have bigger errors than the two

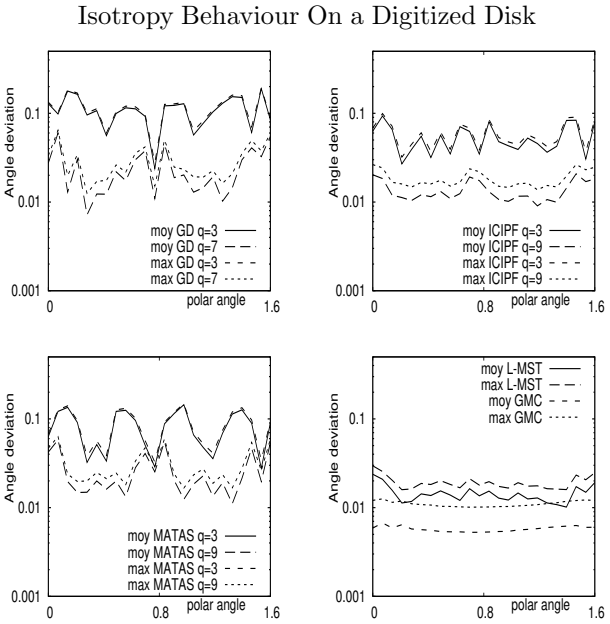

Criterion	GD	ICIPF	MATAS	λ-MST	GMC
Isotropy	-	=	-	+	++

Fig. 8. Test shape is a circle of radius 1, digitized with a grid step equal to 0.01. For this experiment 100 random shifts of the center of the shape were performed. We plot the absolute average deviation and maximal deviation between estimated tangent orientation and theoretical tangent orientation in log-scale on the y-axis on 23 angular sector covering $\pi/2$. Values are plot as a function of the polar angle and the size of the computation window equals $2q+1$. (Left-top) Tangent orientation obtained using convolutions by the Gaussian derivative σ_q. (Right-top) Tangent orientation obtained using implicit parabola fitting with independent coordinates. (Left--bottom) Tangent orientation obtained using the median filtering. (Right-bottom) Tangent orientation using the λ-MST estimator and the GMC estimator.

digital methods. Moreover the Gaussian derivative and the Matas median filtering technique are not isotropic at all as their behaviour is different for points with a polar angle near $k\pi/4$ compared to the other points, this remark stands both for the average absolute error and the maximal absolute error. On the other hand the independent coordinates implicit parabola fitting is more isotropic as the poor behaviour near quadrant and octant changes is not observed. Eventually the λ-MST method and the GMC method behave more isotropically and have a smaller error both in average absolute and maximal absolute error. Moreover the GMC estimator outperforms in terms of precision the λ-MST (almost by a factor 5!). This clearly reflects that methods using the whole shape geometry are likely to give the best results.

4.1.3. *Perimeter Estimation Using Tangent Orientation*

The computed curvilinear abscissa obtained from the summation of the elementary steps on digital curve is a poor estimation (see [23] for a proof of non convergence for length estimators using fixed-size windows on Euclidean segments). We here use the tangent estimation to compute

Table 1
Evaluation of the average absolute error of perimeter using the $L_{\theta_{TAN}}$ method on the digitization of circle of radius 50 with a grid step equal to one. For this experiment 100 random shifts of the center of the shape were performed. The estimators θ_{TAN} used are the Gaussian derivative, the implicit parabola fitting with independent coordinates, the Matas median filtering technique and the iterated implicit parabola fitting with 10 iterations. The size of the computation window spans from 1 to 64 by power of two. We have also computed the result for the λ-MST and the GMC estimators.

Win.size	GD	ICIPF	MATAS	ITICIPF	λ-MST	GMC
q=1	30.6724	30.6724	27.14933	29.67998	0.50378	0.02553
q=2	26.9072	2.35272	11.32574	4.032775		
q=4	6.46475	0.40573	3.622088	0.897381		
q=8	0.79856	0.11547	1.495153	0.181935		
q=16	0.12082	0.06791	1.336123	0.070328		
q=32	0.05776	0.08221	1.336123	0.145093		
q=64	0.13503	0.24110	1.336123	0.462371		

Absolute Perimeter Deviation On a Digitized Disk

Criterion	GD	ICIPF	MATAS	λ-MST	GMC
Perimeter	+	+	-	=	++

the length of a linel of a digital curve and the perimeter by simple summation. We use the method proposed in [10], Chap. 10, Par. 2.4. This approach consider the local length estimation as the dot product of the estimated normal and the normal of the current linel toward the exterior. For short, if $\theta_{TAN}(C_i)$ is the estimated normal at point C_i, the estimated length, denoted $L_{\theta_{TAN}}(C_i)$, equals $|\cos(\theta_{TAN}(C_i))|$ if the associated linel is horizontal, $|\sin(\theta_{TAN}(C_i))|$ otherwise. We evaluate the absolute error of the perimeter, the chosen test shape is a circle of radius 50, digitized for a grid step equal to 1 with 100 random shifts of the center. Results are shown on Table 1. Perimeter evaluation emphasize that there exists a best window size which is a function of the curvature of the border of the shape. The Gaussian derivative and the independent coordinates implicit parabola fitting present good results for particular window sizes, however the Matas median filtering technique gives poor results : its smallest error is 10 times that of the GD or the ICIPF method. Surprisingly the λ-MST gives average results and the best estimation is clearly made by the global min-curvature estimator, its error being approximately .000081 of the expected perimeter.

4.2. *Multi-grid Analysis*

We here first present various experiments regarding the experimental multi-grid analysis of the maximal absolute error (denoted ME) and the average absolute error (denoted AAE) of tangent orientation on shapes with different curvature variations. On all these experiments, estimators using fixed-size windows clearly appear to be not multi-grid convergent. However using various window size (spanning from 3 to 257) we can infer the behaviour of the fixed size estimators as if they were adaptive, using the optimal win-

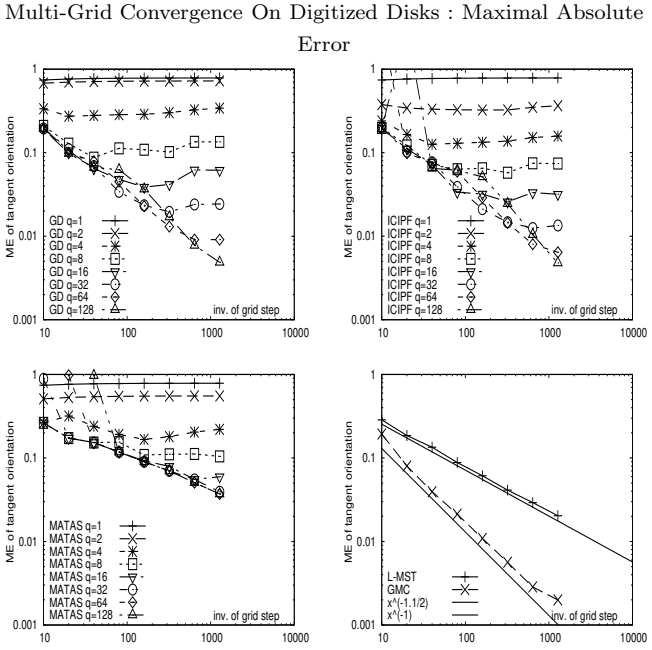

Criterion	GD	ICIPF	MATAS	λ-MST	GMC
Multi-grid Convergence ME on Circle	No	No	No	Yes	Yes

Fig. 9. Multi-grid analysis in log-space : x-axis is the inverse of the grid step, y-axis is the maximal absolute error between theoretical tangent and estimated tangent, the shape of reference is a circle. At each grid step 50 experiments are made and center is shifted randomly. (Left-top) Estimator is the Gaussian derivative. (Right-top) Estimator is the independent coordinates implicit parabola fitting. (Left-bottom) Estimator is the Matas median filtering technique. (Right-bottom) Estimators are λ-MST and Global Min-Curvature, their respective convergence rates are suggested with solid lines.

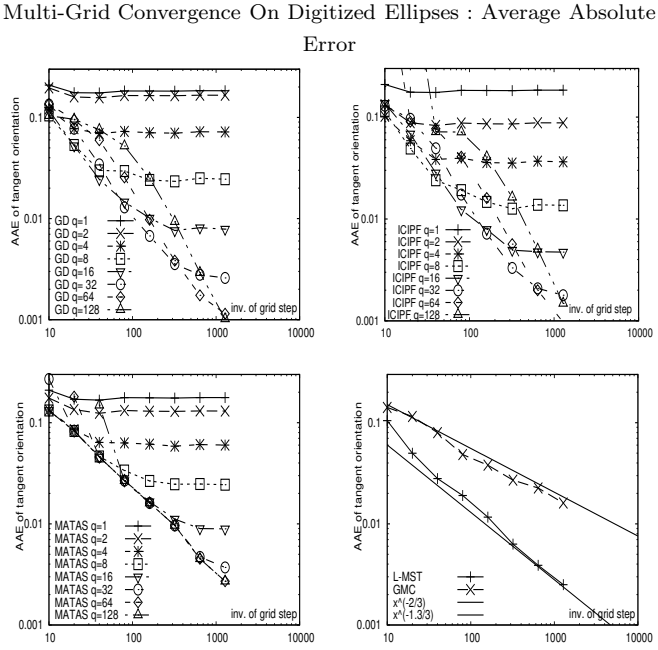

Criterion	GD	ICIPF	MATAS	λ-MST	GMC
Multi-grid Convergence AAE on Ellipse	No	No	No	Yes	Yes

Fig. 10. Multi-grid analysis in log-space: x-axis is the inverse of the grid step, y-axis is the average absolute error between theoretical tangent and estimated tangent, the shape of reference is an ellipse. At each grid step 50 experiments are made and center is shifted randomly. (Left-top) Estimator is Gaussian derivative. (Right-top) Estimator is the independent coordinates implicit parabola fitting. (Left-bottom) Estimator is median filtering. (Right-bottom) Estimator are λ-MST and Global Min-Curvature their respective convergence rates are suggested with solid lines.

dow size at each grid step.

We are first interested in the ME of tangent orientation on the digitizations of a circle, illustrated on Fig. 9. Regarding the maximal absolute error, it is clear that the both of the discrete methods seems uniform multi-grid convergent, the global optimisation method GMC seems to converge in $\mathcal{O}(1/h)$ which is much faster than the λ-MST which seems to converge in $\mathcal{O}((1/h)^{1.1/2})$. The very good results of the GMC estimator are probably due to the fact that the underlying test shape has constant curvature, which makes easier the optimisation process. It is also clear that fixed-size window estimators are not multi-grid convergent even if for each resolution, a suitable window size can be found, in the case of the Gaussian derivative the best reachable precision is in $\mathcal{O}((1/h)^{2.5/3})$. Let us remark that among the fixed-size estimators the Matas median filtering technique has the poorer behaviour.

Let us consider now the AAE of tangent estimation on an ellipse, this time the shape has a smooth curvature variation within positive bounds, results are presented on Fig. 10. The fixed size windows estimators are more or less equivalent, except for the MATAS estimator which seems to be slightly less precise. Surprisingly the GMC estimator is not as efficient as on the circle, even if it still seems multi-grid convergent. The possible reason being the curvature variations of the real underlying shape, indeed the GMC estimator will consider that the underlying shape which minimizes its squared curvature is not an ellipse. As a result the λ-MST seems to be the better choice for curves with smooth curvature variations within positive bounds.

Eventually we consider the AAE of tangent estimation on a test shape with huge curvature variations within opposite signed bounds : the flower, see Fig. 11 for the results. Even though the test shape has much more abrupt curvature variations, the results for the fixed-size estimators are very similar to the ones obtained with the ellipse in terms of best precision. However we can also clearly see that if the computation windows does not suit the geometry of the shape then huge errors will be produced. For example with a window size of 257 points, the Gaussian derivative has an average error which equals almost 1 for grid step 1/10, 1/20, 1/40 and 1/80. For smaller grid steps the error diminishes but is still above the error of all the other window sizes. Same remark applies to the ICIPF estimator and the Matas median filtering technique. Again we also observe that the discrete methods seems multi-grid convergent, the λ-MST

Multi-Grid Convergence On Digitized Flowers : Average Absolute Error

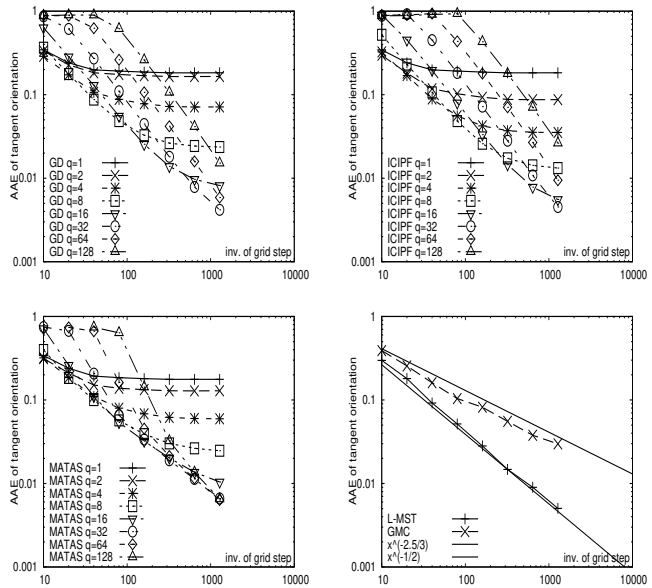

Criterion	GD	ICIPF	MATAS	λ-MST	GMC
Multi-grid Convergence AAE on Flower	No	No	No	Yes	Yes

Fig. 11. Multi-grid analysis in log-space: x-axis is the inverse of the grid step, y-axis is the average absolute error between theoretical tangent and estimated tangent, the shape of reference is a flower. At each grid step 50 experiments are made and center is shifted randomly. Left-top : The estimator is the Gaussian derivative. (Right–top) The estimator is the independent coordinates implicit parabola fitting. (Left-bottom) The estimator is the median filtering technique. (Right-bottom) The estimators are the λ-MST and the GMC, their respective convergence rates are suggested with solid lines.

Asymptotic Behaviour : Average Absolute Error By Time on Circle

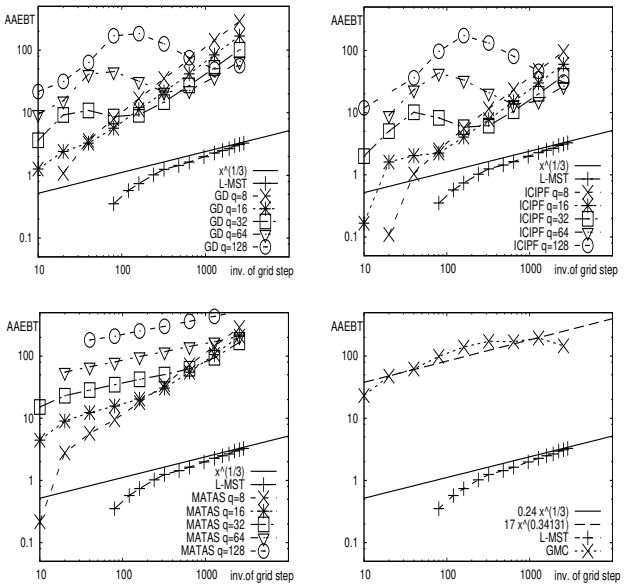

Criterion	GD	ICIPF	MATAS	λ-MST	GMC
As. Behaviour AAEBT on Circle	$\mathcal{O}\left(\frac{1}{h}\right)$	$\mathcal{O}\left(\frac{1}{h}\right)$	$\mathcal{O}\left(\frac{1}{h}\right)$	$\mathcal{O}\left((\frac{1}{h})^{\frac{1}{3}}\right)$	$\mathcal{O}\left((\frac{1}{h})^{0.34}\right)$

Fig. 12. Test shape is a circle of radius 1, the x-axis is the inverse of the grid step. We represent the time spent on computing the tangent field multiplied by the average absolute error between true tangent orientation and estimated tangent. Plots are drawn in the log-space. For fixed size estimators, their asymptotic law seems to be linear with the inverse of the grid step after some rank. For the λ-MST estimator, the asymptotic law seems to be in $\mathcal{O}\left((\frac{1}{h})^{1/3}\right)$ and in $\mathcal{O}\left((\frac{1}{h})^{0.34}\right)$ for the GMC estimator. (Top-left) Estimator is the Gaussian compared to the λ-MST estimator. (Top-right) Estimator is the implicit parabola fitting with independent coordinates compared with the λ-MST estimator. (Bottom-left) Estimator is the Matas median filtering technique compared with the λ-MST estimator. (Bottom-right) Estimator is the global min-curvature estimator compared with the λ-MST estimator.

being the better of the two.

The previous experiments clearly show the main problem when estimating geometric quantities on digital shapes : there is a limit to the best reachable precision which is a function of the size of the digital object under study.

Let us now recall a criterion introduced in [4] to compare local tangent estimators, called AAEBT. This criterion measure the product of the average absolute error of tangent direction estimation by the computation time for the tangent field on the whole curve, and is measured for each grid step. The aim of this estimator is to penalise estimators which make huge errors on average even if the time required for the computation of the tangent field is linear with the inverse of the grid step. Moreover this criterion also penalizes multi-grid convergent estimators that require too many computations. Estimators that have an AAEBT which follows an asymptotic law in $\mathcal{O}((1/h)^{\alpha})$ with $0 < \alpha < 1$ are by definition multi-grid convergent. As problem (2) penalizes estimators using fixed size windows on curves with huge curvature variations we ran the experiments regarding the AAEBT on digitizations of a disk, with 50 random shifts of the center of the shape. The experiments on Figure 12 clearly show that criterion AAEBT for the fixed-size window estimators becomes linear with the inverse of the grid step after some rank, since they reach their best achievable precision. However, judging from the experiments, the λ-MST estimator has a much better AAEBT which seems to be in $\mathcal{O}((1/h)^{1/3})$. This behaviour is consistent with the average absolute error of the tangent orientation in $\mathcal{O}(h^{2/3})$ and the computational cost in $\mathcal{O}(1/h)$ (see [4] for time experiments and [13] for proofs). The GMC estimator seems experimentally to be in $((\frac{1}{h})^{0.34})$), but has an AAEBT which is at about 70 times the one of the λ-MST, indicating that the global optimization scheme is costly compared to the digital straight segment recognition.

4.3. *Improving Continuous Estimators Using Fixed-size Windows*

Preceding experiments have shown that to achieve multi-grid convergence, the size of the computation window should increase with the inverse of the grid step. Experiments using a circle as a test shape with the Gaussian

Size of Computation Window Required to Reach Best Accuracy for Average Absolute Error on Circle

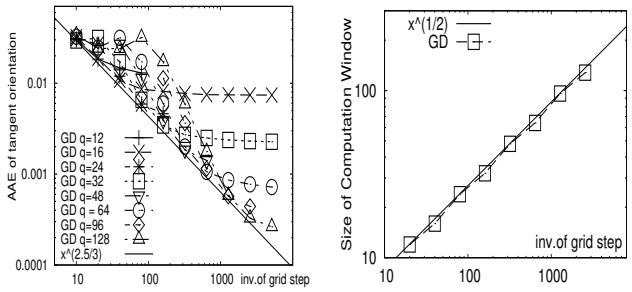

Fig. 13. (Left) Suggested best possible average absolute error with the Gaussian derivative estimator as being some $\mathcal{O}\left((\frac{1}{h})^{5/6}\right)$, with parameter $\sigma = (2q+1)/3$. The test shape is a circle of radius one. (Right) The suggested size of the computation window to achieve best possible accuracy is in $\mathcal{O}\left((\frac{1}{h})^{1/2}\right)$ in the case of a circle of radius one and the Gaussian derivative estimator.

derivative estimator, show that its best possible accuracy is in $\mathcal{O}(h^{5/6})$ provided the size of the computation window follow $\mathcal{O}((1/h)^{1/2})$ as shown on Figure 13.

Unfortunately, we do not know any digital primitive growing at such a speed though we believe that the digital length of circular arcs should follow a $\mathcal{O}((1/h)^{1/2})$ law, yielding the desired computation window to reach the best possible accuracy. Nonetheless the maximal segments can be used to propose new computation windows for fixed-size estimators. To define them let us introduce the functions $B(\cdot)$ and $F(\cdot)$. For a point C_j on the border of a digital shape, $B(C_j)$ is the point C_i, $i < j$ with the smallest index i possible such that $C_{i,j}$ is a digital straight segment. Similarly $F(C_j)$ is the point C_k, $j < k$ with the biggest index k possible such that $C_{j,k}$ is a digital straight segment. We propose seven different computation windows:

$$
\begin{aligned}
q_{1-0} &= max(||B(C_j)) - C_j||_1, ||F(C_j)) - C_j||_1), \\
q_{1-1} &= min(||B(C_j)) - C_j||_1, ||F(C_j)) - C_j||_1), \\
q_{1-2} &= (q_{1-0} + q_{1-1})/2, \\
q_2 &= \left\lfloor q_{1-0}(1/h)^{1/6} \right\rfloor, \\
q_3 &= \left\lfloor (\textstyle\sum_i ||MS_i||_1)/nb(MS_i) \right\rfloor, \\
q_4 &= \left\lfloor \left((\textstyle\sum_i ||MS_i||_1)/nb(MS_i)\right)^{3/2} \right\rfloor, \\
q_5 &= \lfloor (||F(C_j)) - B(F(C_j))||_1 - 1)/2 \rfloor .
\end{aligned}
$$

The q_3 window represents the average length of the maximal segments on the digital boundary and the q_5 window starts from $B(F(PTj))$. The defined windows are either local of global adaptive and their average sizes can be deduced since we know the average size of maximal segments and some of them should grow in $\mathcal{O}\left((1/h)^{1/2}\right)$; Table 2 gathers the adaptivity and expected sizes.

We focus on the behaviour of the Gaussian derivative when using the proposed windows, results are presented in Fig. 14. First of all, on Fig. 14 (a) and (b), regarding the false concavity detection, H1-0 GD, H2 GD, H3 GD, H4 GD and H5 GD seems to behave correctly, although H5 makes a huge error in its estimation compared with the others. In fact H5 GD tends to polygonize the digital curve under study. On Fig. 14 (c), (d) and (e), the poor isotropic

Table 2
Adaptivity of the seven proposed computation windows and their expected average size as a function of the inverse of the grid step.

Window	Adaptivity	Average Expected Size
q_{1-0}	Local	$\mathcal{O}\left((\frac{1}{h})^{\frac{1}{3}}\right)$
q_{1-1}	Local	$\mathcal{O}\left((\frac{1}{h})^{\frac{1}{3}}\right)$
q_{1-2}	Local	$\mathcal{O}\left((\frac{1}{h})^{\frac{1}{3}}\right)$
q_2	Local	$\mathcal{O}\left((\frac{1}{h})^{\frac{1}{2}}\right)$
q_3	Global	$\mathcal{O}\left((\frac{1}{h})^{\frac{1}{3}}\right)$
q_4	Global	$\mathcal{O}\left((\frac{1}{h})^{\frac{1}{2}}\right)$
q_5	Local	$\mathcal{O}\left((\frac{1}{h})^{\frac{1}{3}}\right)$

behaviour of the Gaussian derivative does not benefit from the proposed windows. The perimeter evaluation gets better, being better than the λ-MST except for H1-1 GD and H5 GD, H3 GD being very close to the best value obtained with $q = 32$ and. On Fig. 14 (f) the multi-grid convergence with the ME on the circle bring the uniform convergence for all hybrid estimators except for the H1-1 GD. This is explained by the huge error near quadrant changes already observed for the false concavities detection. We distinguish two extremal convergence speeds, one in $\mathcal{O}(1/h)^{1/2}$ with the H5 GD estimator which is the slowest, the other one in $\mathcal{O}(1/h)^{2.5/3}$ with the H2 GD estimator which is the fastest. The convergence rates obtained with the q_{1-0}, q_{1-2}, q_3 and q_4 window sizes are in-between the ones obtained for q_5 and q_2 window sizes. Experimentally, the convergence rate achieved with the q_2 window size is the best reachable for the Gaussian derivative estimator regarding the ME on the circle. On Fig. 14 (g) hybrid estimators have two behaviours, either $\mathcal{O}(1/h)^{1/2}$ for H4 GD and H5 GD, or $\mathcal{O}(1/h)^{2.7/3}$ for all the others. Eventually on Fig. 14 (h) hybrid estimators are between two behaviours: $\mathcal{O}(1/h)^{1.23/2}$ for H4 GD and $\mathcal{O}(1/h)^{2.7/3}$ for H1-x GD and H3 GD.

Moreover the multi-grid convergence of the Gaussian estimator using the q_5 window can be proved. This is done in two steps : first we show that our discrete convolution on the border of a digital straight line behaves as expected, then we relate our adaptive size of computation window to the growth of maximal digital straight segments (see [5] for technical proofs).

Lemma 1 *If* $\mathbf{C}$ *is a 4-connected digital straight line with rational slope* $\frac{a}{b}$ *then the quantity* $\frac{\hat{C'_y}(k)}{\hat{C'_x}(k)}$ *with* $\hat{\mathbf{C}}'_k = \sum_{i=-q}^{q} G'_{\sigma_q}(-i)\mathbf{C}_{k+i}$ *converges toward* $\frac{a}{b}$ *with an error term in* $\mathcal{O}\left(\frac{1}{q}\right)$.

PROOF. We here consider a and b to be positive integers. $\mathbf{C}$ is a 4-connected digital straight line with rational slope $\frac{a}{b}$ and thus can be parametrized as $\mathbf{C}_i = \left(i - \lfloor \frac{ai}{a+b} \rfloor + \epsilon_X, \lfloor \frac{ai}{a+b} \rfloor + \epsilon_Y\right)$. The values ϵ_X and ϵ_Y rep-

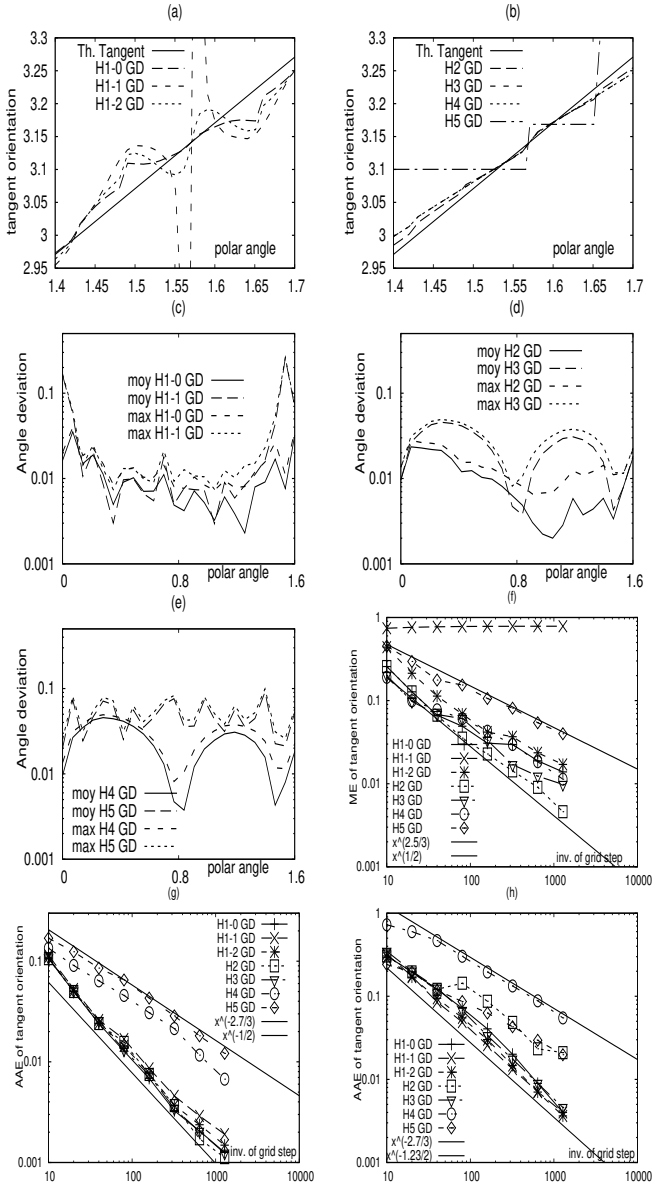

Criterion	H1-0	H1-1	H1-2	H2	H3	H4	H5
Perimeter	0.226	0.808	0.395	0.226	0.0925	0.173	0.761

Fig. 14. Improvements of the Gaussian derivative using the proposed windows. The Estimator called H1-0 GD uses the q_{1-0} window, H1-1 GD uses q_{1-1}, H1-2GD uses q_{1-2}, H2 GD uses q_2, H3 GD q_3, H4 GD uses q_4 and H5 GD uses q_5. (a) & (b) Experiments focus on the false concavity detection for the hybrid estimators. (c) & (d) & (e) Experiments focus on the isotropy behaviour of hybrid estimators. (f) Experiment focuses on the ME for all the hybrid estimators on the circle. The extreme asymptotic laws are suggested with solid lines, in $\mathcal{O}((1/h)^{2/3})$ for the H2 GD estimator and in $\mathcal{O}((1/h)^{1/2})$ for the H5 GD estimator. (g) Experiment focuses on the AAE for the hybrid estimators on the ellipse. Extremal laws are in $\mathcal{O}((1/h)^{2.7/3})$ and in $\mathcal{O}((1/h)^{1/2})$. (h) Experiment focuses on the AAE for the hybrid estimators on the flower. Extremal laws are in $\mathcal{O}((1/h)^{2.7/3})$ and in $\mathcal{O}((1/h)^{1.23/2})$.

resent the possible shifts of the digital line on the digital plane.

We have to evaluate $I_1(q) = \sum_{i=-q}^{q} G'_{\sigma_q}(-i)\lfloor \frac{ai}{a+b} \rfloor$ and $I_2(q) = \sum_{i=-q}^{q} G'_{\sigma_q}(-i)i$ since $\sum_{i=-q}^{q} G'_{\sigma_q}(-i) = 0$.

Let us remark that $\frac{ai}{a+b} - 1 \leq \lfloor \frac{ai}{a+b} \rfloor \leq \frac{ai}{a+b}$ entails :

$\sum_{i=-q}^{q} G'_{\sigma_q}(-i)\frac{ai}{a+b} - \sum_{i=0}^{q} G'_{\sigma_q}(-i) \leq I_1(q)$ and $I_1(q) \leq \sum_{i=-q}^{q} G'_{\sigma_q}(-i)\frac{ai}{a+b} - \sum_{i=-q}^{0} G'_{\sigma_q}(-i)$

As the above summations are approximations of integrals using the well-known "rectangle method" we can thus infer that :

$$-\sum_{i=0}^{q} G'_{\sigma_q}(-i) = \sum_{i=-q}^{0} G'_{\sigma_q}(-i) = \frac{K_1}{q} + \mathcal{O}\left(\frac{1}{q^2}\right)$$

$$\sum_{i=-q}^{q} G'_{\sigma_q}(-i)\frac{ai}{a+b} = K_2\frac{a}{a+b} + \mathcal{O}\left(\frac{1}{q}\right)$$

$$\sum_{i=-q}^{q} G'_{\sigma_q}(-i)i = K_2 + \mathcal{O}\left(\frac{1}{q}\right)$$

with $K_1 = \frac{3}{2}\frac{\sqrt{2}\left(e^{-\frac{9}{2}}-1\right)}{\sqrt{\pi}}$ and $K_2 = \frac{-3\sqrt{2}e^{-\frac{9}{2}} + erf\left(\frac{3}{2}\sqrt{2}\right)\sqrt{\pi}}{\sqrt{\pi}}$

All computation done, since error terms in $\frac{K_1}{q}$ are absorbed in the $\mathcal{O}\left(\frac{1}{q}\right)$ both on the numerator and the denominator, we find that the quantity $\frac{\hat{C}'_y(k)}{\hat{C}'_x(k)}$ equals :

$$\frac{\frac{K_2 a}{a+b} + \mathcal{O}\left(\frac{1}{q}\right)}{K_2 - \frac{K_2 a}{a+b} + \mathcal{O}\left(\frac{1}{q}\right)} = \frac{a}{b} + \mathcal{O}\left(\frac{1}{q}\right)$$

Theorem 2 *The Gaussian derivative estimator using the q_5 window is multi-grid convergent on average with an error term in $\mathcal{O}\left(\left(\frac{1}{h}\right)^{1/3}\right)$.*

PROOF. The q_5 window is such that the whole computation window ($2 * q_5 + 1$ points) is contained in a maximal segment. As a result, Lemma 1 applies, moreover the slope of maximal segments are known to converge, when the grid step tends toward 0, toward the slope of the real tangent of the underlying shape. More precisely, for a point P on the real underlying shape, the slope of the maximal segments on the boundary of the digital border at grid step h of the shape which have a digital point in the disk centered at P of radius h converge toward the slope of the tangent at point P with an error term following $\mathcal{O}\left(h^{1/3}\right)$ on average. As a result the error term is bounded by $\mathcal{O}(\frac{1}{\frac{1}{h}^{1/3}}) + \mathcal{O}\left(h^{1/3}\right)$, that is $\mathcal{O}\left(h^{1/3}\right)$.

5. Conclusion

The presented experiments have shown how the digital tangent estimator compares to classic continuous methods in the ideal digitization case: they are as precise and they

Table 3
This table sums-up the criteria used in this study for the various estimators reviewed. Legend is as follow: (-) poor behaviour, (=) average behaviour, (+) good behaviour, (++) very good behaviour, (?) not tested. Greyed cells correspond to best value for regular estimators and for hybrid estimators.

Estimators	Create False Concavities	Isotropy	Perimeter	Multi-grid Conv. ME on Circle	Multi-grid Conv. AAE on Ellipse	Multi-grid Conv. AAE on Flower
GD	Yes	-	+	No	No	No
ICIPF	Yes	=	+	No	No	No
MATAS	Yes	-	-	No	No	No
λ-MST	No	=	=	$\mathcal{O}\left(\left(\frac{1}{h}\right)^{\frac{1.1}{2}}\right)$	$\mathcal{O}\left(\left(\frac{1}{h}\right)^{\frac{2}{3}}\right)$	$\mathcal{O}\left(\left(\frac{1}{h}\right)^{\frac{2.5}{3}}\right)$
GMC	No	++	++	$\mathcal{O}(1/h)$	$\mathcal{O}\left(\left(\frac{1}{h}\right)^{\frac{1.3}{3}}\right)$	$\mathcal{O}\left(\left(\frac{1}{h}\right)^{\frac{1}{2}}\right)$
H1-0 GD	No	-	+	Yes	$\mathcal{O}\left(\left(\frac{1}{h}\right)^{\frac{2.7}{3}}\right)$	$\mathcal{O}\left(\left(\frac{1}{h}\right)^{\frac{2.7}{3}}\right)$
H1-1 GD	Yes	-	=	No	$\mathcal{O}\left(\left(\frac{1}{h}\right)^{\frac{2.7}{3}}\right)$	$\mathcal{O}\left(\left(\frac{1}{h}\right)^{\frac{2.7}{3}}\right)$
H1-2 GD	Yes	-	+	Yes	$\mathcal{O}\left(\left(\frac{1}{h}\right)^{\frac{2.7}{3}}\right)$	$\mathcal{O}\left(\left(\frac{1}{h}\right)^{\frac{2.7}{3}}\right)$
H2 GD	No	-	+	$\mathcal{O}\left(\left(\frac{1}{h}\right)^{\frac{2.5}{3}}\right)$	$\mathcal{O}\left(\left(\frac{1}{h}\right)^{\frac{2.7}{3}}\right)$	Yes
H3 GD	No	-	+	$\mathcal{O}\left(\left(\frac{1}{h}\right)^{\frac{2.5}{3}}\right)$	$\mathcal{O}\left(\left(\frac{1}{h}\right)^{\frac{2.7}{3}}\right)$	Yes
H4 GD	No	-	+	Yes	$\mathcal{O}\left(\left(\frac{1}{h}\right)^{\frac{1}{2}}\right)$	$\mathcal{O}\left(\left(\frac{1}{h}\right)^{\frac{1.23}{2}}\right)$
H5 GD	No	-	=	$\mathcal{O}\left(\left(\frac{1}{h}\right)^{\frac{1}{2}}\right)$	$\mathcal{O}\left(\left(\frac{1}{h}\right)^{\frac{1}{2}}\right)$	Yes

Asymptotic Behaviour AAEBT on Circle

GD	ICIPF	MATAS	λ-MST	GMC
$\mathcal{O}\left(\frac{1}{h}\right)$	$\mathcal{O}\left(\frac{1}{h}\right)$	$\mathcal{O}\left(\frac{1}{h}\right)$	$\mathcal{O}\left(\left(\frac{1}{h}\right)^{\frac{1}{3}}\right)$	$\mathcal{O}\left(\left(\frac{1}{h}\right)^{0.34}\right)$

are faster as illustrated by Table 3. This is clearly underlined when using the criterion AAEBT. Furthermore, we have shown how to introduce the adaptive window of digital estimators into continuous estimators to add adaptive properties entailing multi-grid convergence and a general better behaviour. Future works will consider noise in the evaluation. Although defining noise in the discrete world is tricky, we plan to use maximal blurred digital straight segments to take into account distortion in the digital curve. We also plan to evaluate the recently published Brunet-Malgouyres estimator [17].

References

[1] A. Balog, I. Bárány, On the convex hull of the integer points in a disc, in: Proc. Symposium on Computational Geometry (SCG'91), ACM Press, 1991.

[2] F. Cazals, M. Pouget, Estimating differential quantities using polynomial fitting of osculating jets, Computer Aided Geometric Design 22 (2005) 121–146.

[3] D. Coeurjolly, R. Klette, A comparative evaluation of length estimators of digital curves, IEEE Trans. on Pattern Analysis and Machine Intelligence 26 (2) (2004) 252–258.

[4] F. de Vieilleville, J.-O. Lachaud, Experimental comparison of continuous and discrete tangent estimators along digital curves, in: Proc. IWCIA'2008, Buffalo (NY), USA, vol. 4958 of LNCS, 2008.

[5] F. de Vieilleville, J.-O. Lachaud, F. Feschet, Convex digital polygons, maximal digital straight segments and convergence of discrete geometric estimators, Journal of Mathematical Imaging and Vision 27 (2) (2007) 139–156.

[6] I. Debled-Rennesson, F. Feschet, J. Rouyer-Degli, Optimal blurred segments decomposition of noisy shapes in linear times, Computers and Graphics 30 (1) (2006) 30–36.

[7] F. Feschet, L. Tougne, Optimal time computation of the tangent of a discrete curve: application to the curvature, in: Proc. DGCI'1999, Marne-La-Vallée, France, vol. 1568 of LNCS, Springer Verlag, 1999.

[8] M. N. Huxley, J. Zunic, Different digitisations of displaced discs, Found. Comput. Math. 6 (2) (2006) 255–268.

[9] B. Kerautret, J.-O. Lachaud, Robust estimation of curvature along digital contours with global optimization, in: Proc. of Discrete Geometry for Computer Imagery, 2008, Lyon, France, vol. 4992 of LNCS, 2008.

[10] R. Klette, A. Rosenfeld, Digital Geometry - Geometric Methods for Digital Picture Analysis, Morgan Kaufmann, San Francisco, 2004.

[11] R. Klette, J. D. Zunic, On discrete moments of unbounded order, in: Proc. DGCI'2006, Szeged, Hungary, vol. 4245 of LNCS, 2006.

[12] J.-O. Lachaud, A. Vialard, F. de Vieilleville, Analysis and comparative evaluation of discrete tangent estimators, in: Proc. DGCI'2005, Poitiers, France, vol. 3429 of LNCS, 2005.

[13] J.-O. Lachaud, A. Vialard, F. de Vieilleville, Fast, accurate and convergent tangent estimation on digital contours, Image and Vision Computing 25 (10) (2007) 1572–1587.

[14] L. Latecki, U. Eckhardt, A. Rosenfeld, Well-composed sets, Computer Vision and Image Understanding 8 (1995) 61:70.

[15] L. J. Latecki, C. Conrad, A. Gross, Preserving topology by a digitization process, Journal of Mathematical Imaging and Vision 8 (2) (1998) 131–159.

[16] T. Lewiner, J. D. Gomes Jr., H. Lopes, M. Craizer, Curvature and torsion estimators based on parametric curve fitting, Computers and Graphics 29 (2005) 641–655.

[17] R. Malgouyres, F. Brunet, S. Fourey, Binomial convolutions and derivatives estimation from noisy discretizations, in: Proc. DGCI'2008, Lyon, France, vol. 4992 of LNCS, 2008.

[18] M. Marji, On the detection of dominant points on digital planar curves, Ph.D. thesis, Wayne State University, Detroit, Michigan (2003).

[19] J. Matas, Z. Shao, J. Kittler, Estimation of curvature and tangent direction by median filtered differencing, in: Proc. of 8th International Conference on Image Analysis and Processing, 1995.

[20] F. Mokhtarian, A. K. Mackworth, Scale-based description and recognition of planar curves and two-dimensional shapes, IEEE Transactions on Pattern Analysis and Machine Intelligence 8 (1) (1986) 34–43.

[21] W. H. Press, B. P. Flannery, S. A. Teukolsky, W. T. Vetterling, Numerical Recipes in C: The Art of Scientific Computing, 2nd ed., Cambridge University Press, Cambridge (UK) and New York, 1992.

[22] B. K. Ray, R. Pandyan, Acord — an adaptive corner detector for planar curves, Pattern recognition 36 (2003) 703–708.

[23] M. Tajine, A. Daurat, On local definitions of length of digital curves, in: Proc. DGCI'03 Naples, Italy, vol. 2886 of LNCS, Springer, 2003.

[24] A. Vialard, Geometrical parameters extraction from discrete paths, in: Proc. DGCI'1996, Lyon, France, vol. 1176 of LNCS, Springer, 1996.

[25] A. P. Witkin, Scale-space filtering., in: 8th Int. Joint Conf. Artificial Intelligence, vol. 2, Karlsruhe, 1983.